Modern Pathology (2020) 33:2580–2590
https://doi.org/10.1038/s41379-020-0607-z

ARTICLE

Molecular characterization of chromophobe renal cell carcinoma reveals mTOR pathway alterations in patients with poor outcome

Juan María Roldan-Romero[1] · María Santos[1] · Javier Lanillos[1] · Eduardo Caleiras[2] · Georgia Anguera[3] · Pablo Maroto[3] · Jesús García-Donas[4] · Guillermo de Velasco[5] · Ángel Mario Martinez-Montes[1] · Bruna Calsina[1] · María Monteagudo[1] · Rocío Letón[1] · Luis Javier Leandro-García[1] · Cristina Montero-Conde[1] · Alberto Cascón[1,6] · Mercedes Robledo[1,6] · Cristina Rodriguez-Antona[1,6]

Received: 8 November 2019 / Revised: 12 June 2020 / Accepted: 13 June 2020 / Published online: 2 July 2020

Abstract

Chromophobe renal cell carcinoma (chRCC) is a histologically and molecularly distinct class of rare renal tumor. TCGA studies revealed low mutational burden, with only *TP53* and *PTEN* recurrently mutated, and discovered alterations in *TERT* promoter and in the electron transport chain Complex I genes. However, knowledge on drug targetable genes is limited and treatments at metastatic stage do not follow a molecular rationale. In a large series of 92 chRCC enriched with metastatic cases, we performed an in-depth characterization of mTOR pathway alterations through targeted NGS and immunohistochemistry (IHC) of phospho-S6, tuberin, and PTEN. Mutations in mitochondria, telomere maintenance and other renal cancer related genes and p53 IHC, were also assessed. The impact on metastasis development and disease specific survival was determined, using TCGA-KICH series ($n = 65$) for validation. mTOR pathway mutations (*MTOR, TSC1*, *TSC2*) were present in 17% of primary tumors, most of them being classified as pathogenic. Mutations were associated with positive IHC staining of phospho-S6 and PTEN ($P = 0.009$ and $P = 0.001$, respectively) and with chRCC eosinophilic variant ($P = 0.039$), supporting a biological relevance of the pathway. mTOR pathway mutations were associated with worse clinical outcomes. Survival analysis gave a hazard ratio of 5.5 ($P = 0.027$), and this association was confirmed in TCGA-KICH (HR = 10.3, $P = 0.006$). *TP53* mutations were enriched in metastatic cases ($P = 0.018$), and mutations in telomere maintenance genes showed a trend in the same direction. p53 IHC staining pattern was associated with the underlying *TP53* defect, and negative PTEN IHC staining (82% of cases) suggested PTEN loss as a chRCC hallmark. In conclusion, our study provides with novel genomic knowledge in chRCC and identifies novel markers of poor survival. Furthermore, this is the first study showing that mTOR pathway mutations correlate with poor prognosis, and may help to identify patients with increased sensitivity to mTOR inhibitors.

Introduction

Chromophobe renal cell carcinoma (chRCC) is a subtype of renal cell carcinoma (RCC) that arises from distal regions of the nephron. This rare tumor accounts for 5% of all RCCs and is histologically and molecularly different from other

Supplementary information The online version of this article (https://doi.org/10.1038/s41379-020-0607-z) contains supplementary material, which is available to authorized users.

✉ Cristina Rodriguez-Antona
crodriguez@cnio.es

[1] Hereditary Endocrine Cancer Group, Human Cancer Genetics Programme, Spanish National Cancer Research Centre (CNIO), Madrid, Spain

[2] Histopathology Core Unit, Spanish National Cancer Research Centre (CNIO), Madrid, Spain

[3] Department of Medical Oncology, Hospital de la Santa Creu i Sant Pau, Barcelona, Spain

[4] Genitourinary and Gynecological Cancer Unit, HM Hospitales—Centro Integral Oncológico HM Clara Campal, Madrid, Spain

[5] Department of Medical Oncology, Hospital Universitario 12 de Octubre, Madrid, Spain

[6] Centro de Investigación Biomédica en Red de Enfermedades Raras (CIBERER), Madrid, Spain

tumor subtypes, such as the clear cell and papillary RCC, which derive from the proximal nephron [1]. ChRCC is subdivided into classic and eosinophilic subtypes, with some morphologic overlap with other entities. ChRCC usually exhibits an indolent pattern of growth, but metastasis can occur in 5–10% of cases [2]. At metastatic stage, treatment follows the standard of care of clear cell RCC, with antiangiogenics, immunotherapy, and mTOR pathway inhibitors, despite large differences in the molecular alterations among these RCC subtypes (e.g., chRCC has low mutational burden and no alterations in *VHL*) [3]. Indeed, previous RCC clinical trials suggest that the response to mTOR pathway inhibitors is histologic specific [4–7], in some cases with chRCC patients having increased benefit for mTOR inhibitors compared with antiangiogenic therapy.

ChRCC is associated with the Birt–Hogg–Dubé and Cowden syndrome, with germline mutations in *FLCN* and *PTEN*, respectively. In the sporadic presentation, due to chRCC rarity, the molecular knowledge is limited. Major findings derived from The Cancer Genome Atlas kidney chromophobe study (TCGA-KICH, $n = 66$) included a low mutational burden, with only *TP53* and *PTEN* being significantly mutated genes. It also suggested that *TERT* promoter alterations and mutations in mitochondrial DNA, affecting proteins of the electron transport chain, were important drivers of the disease. In a second study, Casuscelli et al. with an independent series of 79 chRCC patients, demonstrated that mutations in *TP53* and *PTEN* and imbalanced chromosome duplication were involved in the metastatic progression of chRCC [8–12]. However, despite these two key studies, chRCC molecular alterations remain poorly defined, especially regarding potential drug targets that could be relevant for treatment selection

Here, we worked with a large series of 92 chRCC, with different tumor stages and enriched in metastatic cases, to molecularly characterize mTOR pathway alterations, together with telomere maintenance-related genes, mitochondrial mutations and relevant RCC related genes, and analyzed its clinical significance.

Materials and methods

Patients

Through the Biobanks of IDIBAPS, IRBLleida (PT13/0010/0014), Santiago and Complejo Hospitalario Universitario de Vigo, integrated in the Spanish National Biobanks Network, XBTC and SERGAS, and the collaboration of the Hospital de la Santa Creu i Sant Pau, 92 chRCC patients with available tumor samples and with clinical follow-up were included in the study (Supplementary Table 1). One of the patients from the series had already been described [13]. The cases were selected to represent diverse tumor stages and were enriched in cases that developed metastasis. Primary tumors were obtained and in three cases both primary tumor and metastasis were available. In total, 95 tumor samples were collected, 78 were formalin-fixed paraffin embedded (FFPE) and 17 were frozen tissues. The characteristics of the patients are summarized in Table 1. A general positive advice for the utilization of the tissue was foreseen by the institutional board. Mutational analysis results were obtained from 87 cases (five cases failed NGS) and immunohistochemistry (IHC) characterization was performed in samples with tumor slides available: 57 (for pS6, PTEN, tuberin) and 39 (for p53) cases.

Table 1 Characteristics of the 92 chRCC patients and tumor samples analyzed.

Characteristics	*n*	(%)
Age at diagnosis (year)		
Median [min, max]	61 [27, 84]	
Gender		
Female	32	35
Male	60	65
Stage at diagnosis		
I	32	35
II	27	29
III	29	32
IV	3	3
NA	1	1
Morphology		
Classic	60	65
Eosinophilic variant	31	34
NA	1	1
Multiple chRCC tumors		
Yes	2	2
No	90	98
Developed metastasis		
Yes	19	21
No	73	79
Tumor samples analyzed		
Primary tumor	92	97
Paired metastasis	3	3
Primary tumors with NGS data		
Yes	87	95
No	5	5
Primary tumors with IHC data		
Yes	57	62
No	35	38

DNA extraction and targeted next generation sequencing

Tumor samples with more than 70% of tumor cells were selected for genomic DNA extraction with the Maxwell® RSC DNA FFPE Kit (Promega) using the Maxwell® RSC Instrument (Promega). DNA from frozen tumor samples was isolated using DNeasy Blood and Tissue Kit (Qiagen) according to manufacturer instructions. Hybridization-based target enrichment of tumor DNA was used to sequence the full coding region plus the splice sites of 42 genes (Supplementary Table 2) plus *TERT* promoter region (250 nucleotides upstream of the translation start site). Fourteen genes were related with mTOR-PI3KCA pathway, 19 were genes recurrently mutated in different RCC histologies, seven were general cancer driver genes, and three genes were associated with telomere maintenance. Briefly, targeted libraries were constructed with 200–250 ng of tumor DNA using the SeqCap EZ Choice Enrichment kit (Roche) and were sequenced and demultiplexed in a MiSeq or HiSeq Illumina sequencer using a 100 paired-end mode, yielding an average of ~3 million read pairs per sample. Demultiplexed raw data in fastQ format was trimmed using Cutadapt software (v.1.16) to remove low quality ends and Illumina's universal adaptor content. Reads were aligned with bwa-mem (v.0.7.17-r1188) using GRCh37/hg19 reference genome. BAM files were sorted using Samtool (v.1.9) and duplicate reads were marked using Picard tools (v.2.18.7). Read depth coverage per sample was obtained using Picard hsmetrics tool. A median coverage depth ≥50 was required to include the sample in the study. The average median bait coverage of the 90 samples (87 primary tumors and 3 paired metastasis) was 236× (minimum of 55, maximum of 748; interquartile range 126–405). The on-target (plus ± 100 bp padding around the targeted regions) somatic variant calling was done using Mutect2 from GATK (v.4.0.5.1) in tumor-only mode. The variants present in gnomAD (https://gnomad.broadinstitute.org/) with an allele frequency (AF) > 0.0001 were not considered further, as they were potentially germline. Coding non-synonymous and loss-of-function (LOF) variants (labeled as Moderate or High Impact by VEP; e.g., missense, nonsense, those disrupting canonical splice sites, inframe, and frameshift indels) with a variant AF ≥ 0.15 and with 3 or more alternative reads supporting the variant were considered for the analysis. Mutations with an AF > 0.60 were considered indicative of loss of heterozygosity (LOH), except those in X chromosome for male patients.

Somatic variants in the mitochondrial DNA (MT-DNA) were detected using off-target reads from the panel, following a similar variant calling and annotation strategy as mentioned above. Samples with a MT-DNA coverage depth <10 were not included in the analysis, and we focused in variants with high heteroplasmy. The median coverage in the mitochondrial chromosome of the analyzed samples was 46× (minimum of 13, maximum of 285; interquartile range 28–76). Variants detected in a panel of normals and repetitive variants (detected in ten or more independent samples and classified as artefacts) were filtered out. We applied the same filters as TCGA-KICH project [10] to include mitochondrial variants in the analysis (i.e., LOF variants with heteroplasmy ≥ 0.75).

Immunohistochemistry analysis

FFPE tumor sample sections were hematoxylin and eosin (H&E) stained and two representative areas of each tumor were included as 1 mm diameter cores in tissue microarrays. For different staining methods, slides were deparaffinized in xylene and rehydrated through a series of graded ethanol until water. Consecutive sections were stained with H&E, and several IHC reactions were performed in an automated immunostaining platform (Autostainer Link 48, Dako; Bond Max II, Leica, just in case of phospho-S6). Antigen retrieval was first performed with the appropriate pH buffer (Low pH buffer, Dako; ER1, Bond; High pH buffer for p53) and endogenous peroxidase was blocked (peroxide hydrogen at 3%). Then, slides were incubated with the appropriate primary antibody as detailed: rabbit polyclonal anti-P-S6 (1/250, cell signaling, #2211), rabbit monoclonal anti-PTEN (138G6, 1/75, Cell Signaling, #9559), rabbit monoclonal anti-tuberin (D93F12, 1/100, Cell Signaling, #4308), and mouse monoclonal p53 FLEX (Clone DO-7 ready-to-use [Link], Dako, #IR616). After the primary antibody, slides were incubated with the corresponding visualization system (EnVision FLEX+, Dako; Bond Polymer Refine Detection, Bond, Leica for p53) and conjugated with horseradish peroxidase. Immunohistochemical reaction was developed using 3,3′-diaminobenzidine tetrahydrochloride (DAB) and nuclei were counterstained with Carazzi's hematoxylin. Finally, the slides was dehydrated, cleared and mounted with a permanent mounting medium for microscopic evaluation.

A pathologist (EC) evaluated, blinded to the clinical data, the intensity and extension of the staining in the tumor cells and categorized cases as pS6 and PTEN expressors/non-expressors by scoring the staining intensity in the cytoplasm as absent, weak, moderate, or strong. Expressors were those tumors with moderate/strong-positive staining; non-expressor tumors were those with absent/weak intensity. Tuberin expression levels (corresponding to *TSC2* gene) were assessed scoring the staining intensity in the cytoplasm and the membrane categorizing cases as: absent, weak, or strong staining. The staining pattern of p53 was evaluated in tumors with whole sections available and classified based on previously described criteria for ovarian carcinoma [14],

using a cutoff value of 30%. Staining was classified as: complete absence, tumors completely negative (0% cells staining) with positive stromal cells serving as internal positive control; wild-type pattern, ≤30% of tumor nuclei showed positivity; overexpression, >30% of tumor nuclei showed positivity. For tumors with ≤30% positive nuclei, staining was also compared with non-tumoral kidney, if present in the slide, to avoid misinterpretation due to fixation issues [15]. Representative IHC images are shown in Figs. 2, 3 and Supplementary Fig. 1.

Statistical analysis

Associations between mutations and IHC staining were analyzed using Pearson's Chi-square test, and logistic regressions were used for the reverse phase protein array (RPPA) data from TCGA. Binary logistic regressions were used to analyze the association between eosinophilic variant and mutations. Logistic regressions were used to analyze the association between the mutations/IHC staining and the development of metastasis. Cox regression analyses and Kaplan–Meier survival analysis were employed to analyze the association between the mutations/IHC markers and the disease specific survival (DSS) of the patients. DSS was defined as the time between the date of chRCC diagnosis and the date of death from the disease or last documented follow-up. Multivariable analysis included as covariates tumor stage, gender, and age at chRCC diagnosis.

An exploratory analysis was performed with the patients included in this study, with P values < 0.05 considered significant, and TCGA-KICH series [10, 11] was used for validation. SPSS version 19.0 was used for statistical analysis. Data visualization was performed with Oncoprint and ggplot2 packages in R version 4.0.

Relevant demographic and clinical data from patients, mutations and IHC results, are provided in Supplementary Table 1.

Results

Clinical characteristics of patients

Among the 92 chRCC patients included in the study, 60 (65%) were men and had a median age of diagnosis of 61 years old. Cases were selected to represent various tumor stages and the series was enriched in patients that developed metastasis. Thus, 32 (35%) of tumors corresponded to stage I disease, 27 (29%) to stage II, 29 (32%) to stage III, and 3 (3%) were metastatic at diagnosis; with 19 patients (21%) developing metastasis. 31 patients (34%) had eosinophilic variant of chRCC. Median DSS of the patients was not reached, the first quartile survival (75% cumulative survival) was 14.6 years. A full description of the characteristics of the patients is provided in Table 1.

Mutational landscape of chRCC

As shown in Fig. 1, *TP53* was the most frequently altered gene in chRCC primary tumors, with 26 out of 87 cases mutated (30%), similarly to TCGA KICH and Casuscelli et al. [10–12]. In eight cases LOH was detected, and in two cases two different mutations were present in the same tumor, suggesting convergent mutation evolution.

MTOR was mutated in 9% of primary tumors (8 of 87), in all cases with allele frequencies consistent with activating variants present in one allele. Among the mutations detected, four have been described as activating (p.S2215F, p.I2500F, p.I2501F, and p.V2006F [16, 17]), one detected in three tumors is located in the kinase domain of mTOR (p.L2427R), and one is a novel mutation (p.E1613Q). When considering other variants affecting mTOR pathway, six patients (7%) carried *TSC2* mutations, two of them with several mutations in the tumor (one with three and another with two mutations, Fig. 1), and among the nine *TSC2* mutations detected, four were LOF. One tumor carried a *TSC1* LOF mutation. Thus, most mutations in *MTOR, TSC1*, and *TSC2* were pathogenic variants, with only three tumors carrying variants of unknown significance. In total, mTOR pathway alterations in *MTOR, TSC1*, and *TSC2* genes were present in 15 out of 87 primary tumors (17%). Mutations in other genes related with PI3K-AKT-mTOR pathway were also found: two variants in *STK11* and *PIK3C2B* genes and single mutations in *AKT2*, *DEPDC5*, *PIK3CA, RPTOR*, and *RICTOR* genes. Most of these were missense variants of unknown significance.

PTEN and *FLNC* were found mutated in four and three patients, respectively. Regarding telomere maintenance-related genes, *TERT* promoter C228T mutation was found in five patients, and *ATRX* and *DAXX* mutations were found in five and three cases, respectively. One of the *ATRX* and two the *DAXX* mutations were LOF variants. Combined, 14% of patients had alterations in these telomere-related genes. Chromatin remodeler genes (most frequently *ARID1A*), and the deubiquitinase *USP9X* were also mutated in some tumors.

TCGA showed that MT-DNA genes that encode for the complex I of the electron respiratory chain are frequently mutated in chRCC [10]. In our study mitochondrial LOF mutations with >75% heteroplasmy were detected in these genes in 15% (14 of 73) of primary tumors (Supplementary Table 1). Eight of these mutations affected *MT-ND4*. Three were single nucleotide nonsense variants, four were short indels in non-homopolymeric regions and six were indels in homopolimeric tracks (one present in two samples), in all

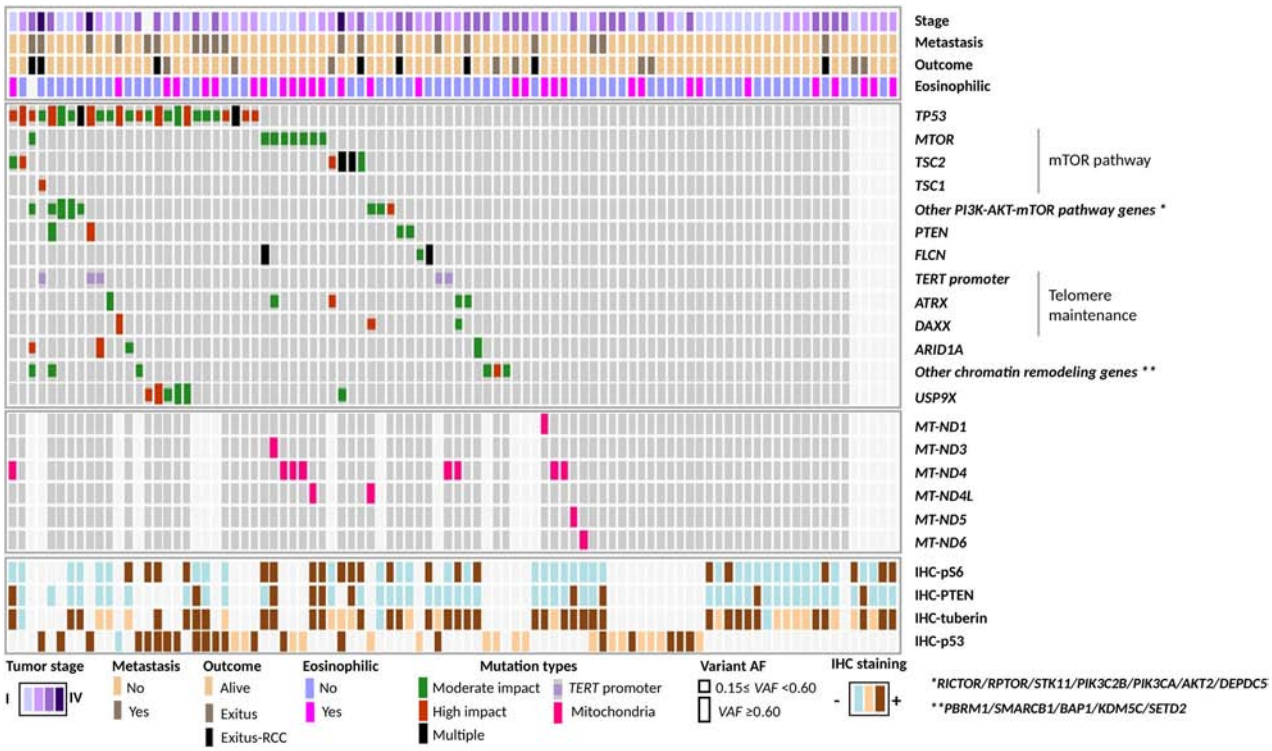

Fig. 1 OncoPrint plot showing mutations found in the chRCC tumors together with IHC stainings. The matrix shows the 92 primary tumors analyzed in the series. The upper rows indicate characteristics of the cases (stage, metastasis, survival outcome, and eosinophilic variant). The rows in the middle panels show mutations colored according to the variant impact (high or moderate); black boxes denote cases with multiple mutations in the gene. Those variants with an allele fraction (AF) above 0.60 are depicted by long bars, while lower frequencies are represented by squares. Mitochondrial DNA mutations are shown in pink. The last panel shows IHC results for phospho-S6 (S235/236), PTEN, tuberin, and p53 proteins. Colors indicate different IHC staining categories (blue–brown) as defined in "Methods" section.

cases previously observed in chRCC or oncocytoma [10, 18].

In our series, there were three cases with both primary tumor and metastasis available. The mutations and allele frequencies detected in these matched samples was similar (Supplementary Table 1). Representative photomicrographs of tumors with different molecular alterations is presented in Supplementary Fig. 2.

Correlation between mTOR pathway mutations and IHC for pS6, PTEN, and tuberin

Regarding mutational events, pS6 IHC revealed a positive staining in 37% (21 of 57) of the chRCC tumors, and the rate of positive staining was almost threefold increased in tumors with mTOR pathway mutations compared with wild-type tumors (70% versus 26%, $P = 0.009$; Fig. 2a). The protein RPPA data from TCGA-KICH supported this association ($P = 0.028$ data not shown). PTEN negative IHC staining was observed in 82% of cases, and was more frequent in cases wild-type for *MTOR, TSC1*, or *TSC2* genes than in mutated tumors ($P = 0.001$; Fig. 2b), supporting independent events converging on PI3K-AKT-mTOR pathway. As expected, tuberin staining was associated with LOF mutations in *TSC2* gene ($P = 0.020$, Fig. 2c). IHC staining of these proteins was not associated with the clinical characteristics of the patients nor with the tumor stage.

chRCC eosinophilic variant is associated with mutations in mTOR pathway and in the electron transport chain complex I genes

When the tumor mutations were compared with chRCC eosinophilic variant, an association was found for mTOR pathway (*MTOR*, *TSC1*, and *TSC2*) and for the mitochondrial genes encoding the complex I of the electron respiratory chain. The eosinophilic variant occurred more frequently in tumors with mTOR pathway mutations (57% versus 28%; OR = 3.5 with $P = 0.039$) and in tumors with MT-DNA mutations in the electron transport chain complex I genes (71% versus 22%; OR = 8.8 with $P = 0.0011$). The MT-DNA coverage also had a positive association with the eosinophilic variant ($P = 0.027$), maybe reflecting the higher number of mitochondria present in this morphology. The mutations in the electron respiratory chain remained

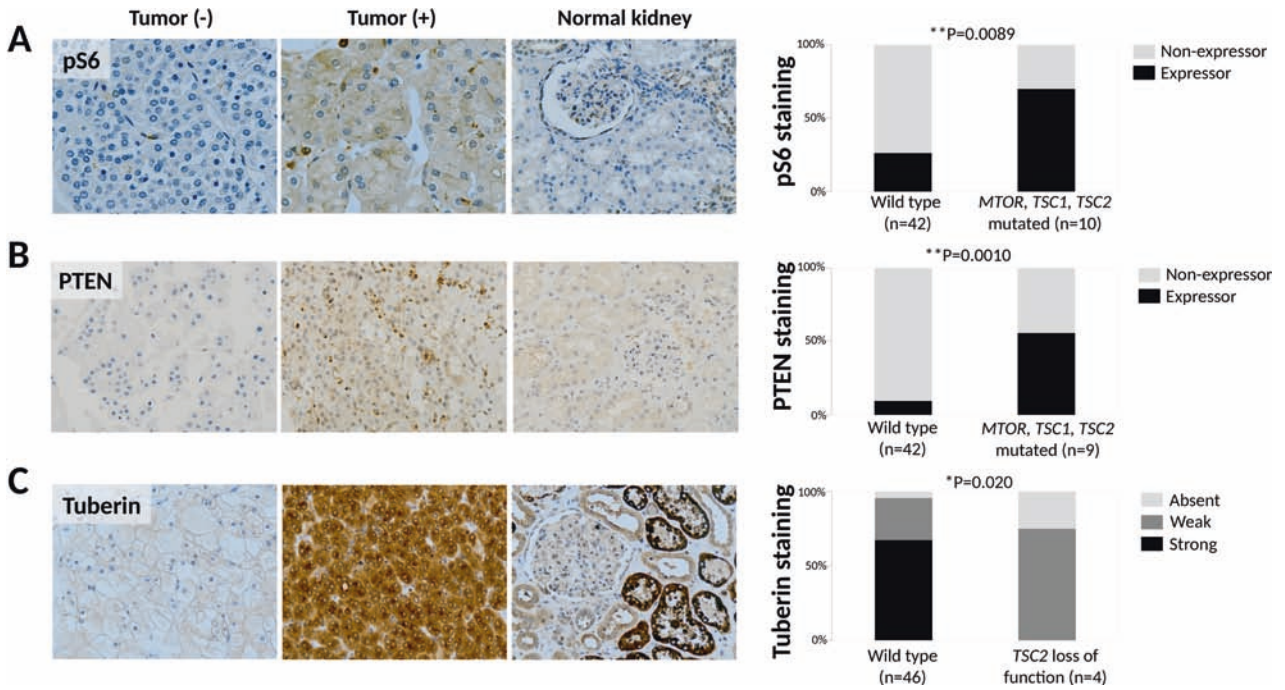

Fig. 2 pS6, PTEN, and tuberin IHC representative images and association with mTOR pathway mutations. IHC stainings for non-expressor and expressor tumors and normal kidney together with bar diagrams showing the percentage IHC classes according to mutations in mTOR pathway for (**a**) pS6 and (**b**) PTEN. Tuberin IHC stainings and bar diagram for *TSC2* LOF mutations (**c**). IHC pictures are shown at ×20 of magnification. Significant *p* values are shown above the graphs. *P* values correspond to Pearson's Chi-square test.

significantly associated with the eosinophilic variant after adjusting for the coverage depth (OR = 5.1, $P = 0.037$).

p53 nuclear accumulation is associated with *TP53* missense mutations

Mutations in *TP53* are associated with poor outcome in chRCC [12]. To investigate whether p53 IHC could serve as a surrogate for *TP53* mutations, we performed IHC and assessed staining differences among the different mutational groups (Fig. 3). p53 overexpression was more frequent in tumors with *TP53* missense mutations than in tumors without *TP53* mutation (89% versus 35%; $P = 0.006$), most of which showed wild-type IHC expression pattern. One tumor with complete absence of p53 expression carried a splice donor mutation with high variant allele fraction (0.78), suggesting LOH. Cytoplasmic pattern of p53 staining was not observed.

Primary tumor alterations and patients' clinical course: metastasis development and disease specific survival

Considering the survival of the patients, we found that *MTOR, TSC1*, or *TSC2* mutations were associated with worse DSS (HR = 5.5, $P = 0.027$, univariate). Multivariable analysis including tumor stage as a covariate, gave similar results (HR = 10.7, $P = 0.031$; multivariable analysis; Table 2). In addition, if only metastatic patients were included in the analysis ($n = 19$), mTOR pathway mutations were again associated with shorter survival times (HR = 12.6, $P = 0.047$; multivariable analysis). In the TCGA-KICH series, mutations in these genes were also associated with poorer DSS (Table 2). Kaplan–Meier curves are presented in Fig. 4. Adding *TP53* mutations as a covariate to the analyses did not substantially change the results. In our series, no other genes were associated with the survival, while in TCGA *TP53* and telomere-related alterations were associated with poor survival of the patients (Table 2). Full details of the association results are presented in Supplementary Table 3.

When the mutations were compared with the development of metastasis, *TP53* alterations were enriched in metastatic cases (OR = 3.6, $P = 0.018$; Table 2) and p53 overexpression assessed by IHC showed a similar association (OR = 8.8, $P = 0.012$). A trend for telomere maintenance genes was found (OR = 3.1, $P = 0.084$). When tumor stage was added as a covariate in these analyses, the association of both *TP53*/p53 IHC and telomere related-genes decreased, indicating these events are not independent. In TCGA-KICH, mutations in mTOR pathway and in telomere maintenance genes were associated with metastasis development ($P = 0.034$ and $P = 0.033$, respectively; Table 2).

A

Immunohistochemical staining pattern of p53	Classification of tumors according to *TP53* mutations				
	Wild type	Missense	Nonsense	Frameshift	Splice site
Overexpression	8	8	2	3	0
Wild type pattern	15	1	1	0	0
Complete absence	0	0	0	0	1
Total	23	9	3	3	1

B

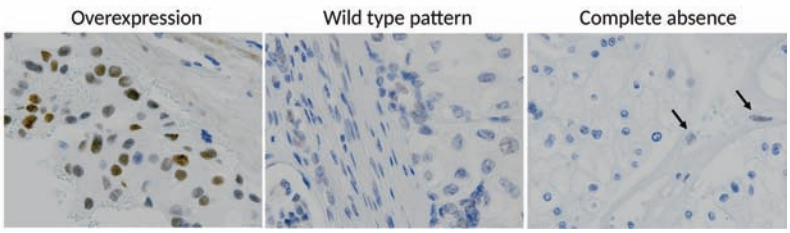

Fig. 3 Immunohistochemical staining pattern of p53 according to *TP53* mutations. **a** Distribution of p53 IHC staining according to *TP53* mutation type. **b** Representative stainings corresponding to tumors with p53 overexpression, wild-type pattern and complete absence. Pictures are shown at ×40 of magnification.

Mutations in other genes and the IHC for pS6, PTEN, or p53 were not associated with metastasis nor with the survival of the patients.

Discussion

chRCC is an uncommon histologic subtype of RCC for which limited molecular knowledge exist and with not well established therapeutic options at metastatic stage. In this study, we combined NGS and IHC techniques to characterize the tumor alterations of the largest series of chRCC described so far. Our results suggest an important biological relevance for mTOR pathway, with *MTOR, TSC1*, and *TSC2* mutations associated with poorer clinical outcomes and distinct morphological features.

TCGA-KICH project with 66 patients was the first in-depth somatic genomic characterization of chRCC, however, histopathologic information was limited [10]. A subsequent study by Casuscelli et al. provided with molecular data for 79 additional chRCC patients [12]. These studies discovered low mutational burden, frequent mutations in *TP53* and *PTEN*, *TERT* dysregulation and mitochondrial DNA alterations, as major hallmarks of the disease. However, mTOR pathway was not studied in detail. Alterations in mTOR pathway (in either *MTOR, TSC1*, or *TSC2*) in our series were present in 17% of primary tumors, compared with 4% and 10% in TCGA and Casuscelli et al. series [10, 12]. The lower frequency of mTOR pathway mutations in TCGA could be explained by the lower depth of coverage associated with whole exome sequencing. Most of the variants detected in our series were pathogenic, consistent with a functional relevance. Furthermore, these mutations were also significantly associated with positive IHC staining for pS6 and PTEN (Fig. 2), in line with activation of downstream effectors, lack of redundancy in the pathway, and supporting mTOR pathway dependence in this subset of tumors. Interestingly, oncocytic renal tumors with unusual morphologic features have been described related with specific molecular defects [19, 20], including somatic *MTOR* and *TSC2* alterations and *TSC1/2* germline mutations [21, 22]. In our series, we find an overrepresentation of the eosinophilic variant of chRCC in mTOR pathway mutated tumors. Regarding the clinical course of the patients, in our series and in TCGA-KICH, these mutations were associated with worse DDS and also with increased metastasis risk in TCGA-KICH series.

TP53 and *PTEN* mutations have been pinpointed as critical events for chRCC metastatic evolution [12]. In this study, we confirmed the association of *TP53* with metastasis development, reinforcing its strong role in tumor progression. We also show that p53 IHC in chRCC is informative of the subjacent *TP53* alteration, suggesting IHC could be used as a surrogate marker of mutations. We did not detect an association between PTEN and metastasis, maybe due to the small number of mutated tumors. This low number of *PTEN* mutated tumors is in contrast with the vast negative PTEN IHC staining we find in our series (5% and 82%, respectively), which suggests that loss of PTEN protein may be a hallmark of chRCC. This is supported by PanCancer-TCGA RPPA data, in which chRCC is the second tumor with the lowest *PTEN* protein expression score among 32 tumor types (Supplementary Fig. 3) [23]. Recent studies in clear cell RCC find a similar, though less pronounced, pattern for *PTEN* mutations and protein expression, with loss of PTEN protein predicting response to mTOR inhibitors [24, 25]. How *PTEN* is downregulated in RCC tumors is still unknown, although epigenetic events have been suggested to play a role in *PTEN* inactivation [26].

When we analysed mutations in other genes, we found that telomere maintenance-related genes, *TERT*, *ATRX*, and *DAXX*, are mutated in 14% of our cases (18% in TCGA-KICH), with *TERT* promoter mutations being mutually exclusive with the other genes, as reported in previous

Table 2 Risk of metastasis and DSS according to molecular characteristics found in the primary tumors.

Characteristic	Metastasis development				Disease specific survival (DSS)			
	This study		TCGA-KICH		This study		TCGA-KICH	
	Univariate OR (95% CI), *P*	Multivariate[a] OR (95% CI), *P*	Univariate OR (95% CI), *P*	Multivariate OR (95% CI), *P*	Univariate HR (95% CI), *P*	Multivariate HR (95% CI), *P*	Univariate HR (95% CI), *P*	Multivariate HR (95% CI), *P*
Mutated gene								
TP53	**3.6 (1.3–10.4), 0.018**	3.6 (0.9–13.8), 0.065	2.6 (0.7–9.3), 0.15	1.0 (0.2–5.4), 0.97	0.8 (0.2–4.2), 0.81	1.4 (0.2–9.1), 0.72	**6.6 (1.3–34.0), 0.025**	3.7 (0.4–33.5), 0.24
MTOR/TSC1/TSC2	1.4 (0.4–5.0), 0.62	1.6 (0.3–7.9), 0.56	**12.9 (1.2–137), 0.034**	**145 (2.5–8491), 0.016**	**5.5 (1.2–24.7), 0.027**	**10.7 (1.2–92.2), 0.031**	**10.3 (2.0–54.8), 0.006**	670 (0.7–603146), 0.060
PTEN	3.9 (0.5–29.6), 0.19	1.1 (0.1–11), 0.94	3.0 (0.6–15.6), 0.19	2.5 (0.2–27), 0.44	2.6 (0.3–21.8), 0.38	1.0 (0.1–8.8), 0.99	3.0 (0.6–15.6), 0.18	0.87 (0.05–14.1), 0.92
Telomere maintenance[b]	3.1 (0.9–11.3), 0.084	3.7 (0.8–17.6), 0.10	**4.9 (1.1–20.9), 0.033**	7.1 (0.9–57.3), 0.065	1.5 (0.3–7.6), 0.62	1.6 (0.3–8.7), 0.62	4.2 (0.9–18.7), 0.062	9.8 (0.8–123.5), 0.077
Complex I resp. chain	3e−9 (NP[d]), 0.999	9e−9 (NP), 0.998	3.5 (0.8–15.6), 0.11	5.3 (0.7–38.5), 0.099	0.04 (0–2630), 0.56	0 (NP), 0.99	2.5 (0.5–13.1), 0.27	1.3 (0.2–9.3), 0.82
Protein expression[c]								
p53 (overexpression)	**8.8 (1.6–48.2), 0.012**	7.3 (0.9–55.9), 0.057			44.2 (NP) 0.66	143.5 (NP), 0.65		
pS6 (S235–S236)	1.1 (0.3–3.9), 0.89	0.6 (0.1–3.3), 0.51	0.6 (0.3–1.6), 0.34	0.7 (0.2–2.4), 0.59	1.5 (0.3–7.7), 0.60	5.8 (0.4–86.4), 0.20	1.3 (0.4–4.4), 0.65	0.6 (0.04–10.5), 0.75

Associations with a P value < 0.05 are given in bold. Full details of the association analysis are provided in Supplementary Table 3.

[a]The analysis includes as covariates: tumor stage, age and gender.

[b]Telomere maintenance-related genes include *TERT* promoter, *ATRX* and *DAXX*.

[c]Protein expression in this study was assessed by IHC, in TCGA study RPPA values were used.

[d]Large confidence interval, not provided (NP).

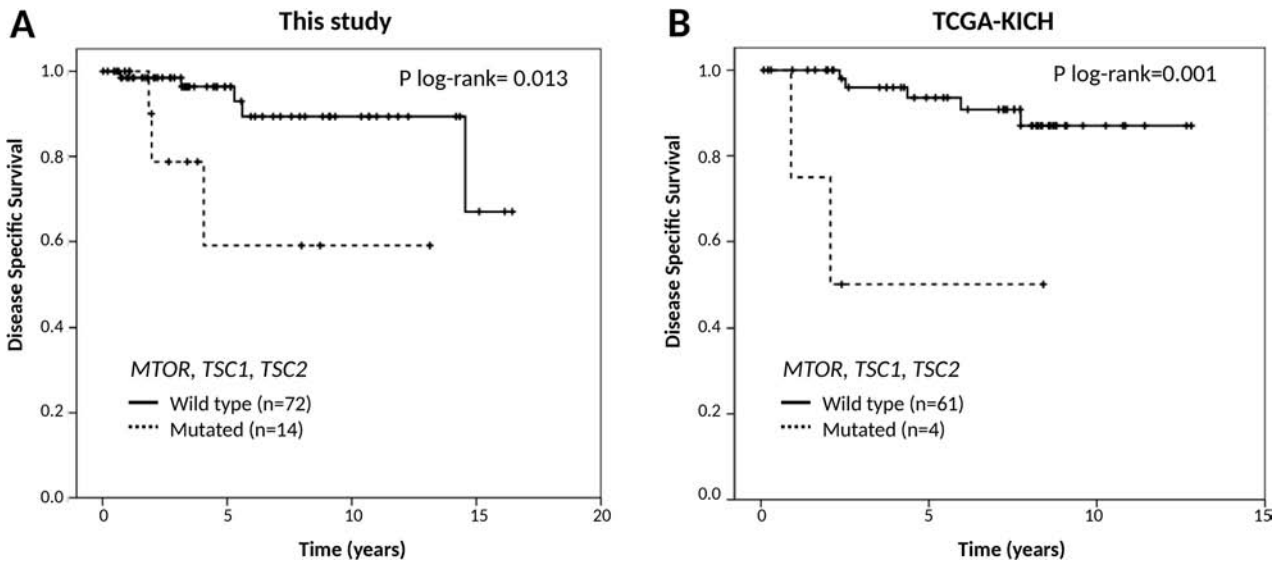

Fig. 4 Impact of mTOR pathway mutations on patient DSS. Survival analysis was performed with patients grouped according to *MTOR/TSC1/TSC2* mutation status in: (**a**) this study and (**b**) in TCGA-KICH. The *P* values included in the graph correspond to the log-rank test.

studies [27]. Our series and TCGA-KICH suggest an increase in telomere-related mutations in metastatic chRCC cases, in agreement with previous studies in non-clear RCC that described *TERT* promoter mutations associated with larger tumors and metastatic development [28]. We found *FLCN* mutations in three cases, while none were detected in TCGA and Casuscelli et al. series [10, 12]. One patient had Birt–Hogg–Dubé syndrome, while this data were not available for the other two cases (a patient diagnosed at age 27 and with a *FLCN* missense mutation of unknown significance and a 75 years old patient carrying two LOF mutations). One patient with bilateral tumors and diagnosed at 75 years carried a *PTEN* missense mutation classified as likely pathogenic in ClinVar (p.V255E; VAF = 0.40), however, neither germline DNA nor additional clinical details were available from this patient. Altogether, this data suggests that hereditary cases might be included in apparently sporadic series of chRCC. Mitochondrial LOF mutations in the electron transport chain Complex I genes were found in 19% of our cases (17% in TCGA-KICH). Comparison analysis among TCGA tumor types using Whole Genome Sequencing data [29] have revealed that chRCC and thyroid cancers are the tumors with the highest proportions of mitochondrial mutations, being transversions particularly high in chRCC patients. We did not find an association between these alterations and the clinical outcome of the patients, however, we uncovered an association with the eosinophilic variant of chRCC tumors, in agreement with results derived from small number of cases [18, 19].

Despite the recent improvement in the molecular knowledge in chRCC, treatments for metastatic stage are still unspecific and unrelated to the molecular defects. The few existing clinical trials on non-clear RCC may suggest that chRCC has improved responses to mTOR inhibitors, compared with antiangiogenics [4–6]. This may reflect the fact that *VHL* mutations, which can explain sensitivity to antiangiogenic drugs in clear cell RCC, are absent in chRCC. Cancer cells with mTOR pathway mutations have a dependency on this signaling, and we and others have shown in large series of RCC patients, mainly with clear cell histology, that mutations in *MTOR, TSC1*, or *TSC2* confer sensitivity to mTOR inhibitors [25, 30]. In this study we show that there is a subset of chRCC cases with mTOR pathway alterations and aggressive tumors associated with worse clinical outcomes. These patients might benefit from mTOR targeted therapies. In this respect, in our chRCC series only two cases with mTOR pathway mutations received mTOR inhibitors, one was uninformative (everolimus for 13 days before exitus), but the other was a case we previously reported, with two *TSC2* mutations and an extraordinary response to temsirolimus. This observation reinforces a link between mTOR pathway mutations and response to rapalogs [13]. However, this hypothesis should be further investigated in metastatic chRCC patients with systemic treatments.

Classification of pink RCC tumors with *MTOR/TSC1/TSC2* mutations is an evolving area, and several recently described distinctive entities that harbor these mutations may overlap with chRCC. Thus, cases with these mutations and classified as chRCC, could potentially be another entity, such as eosinophilic solid and cystic tumors [31, 32] or eosinophilic and vacuolated RCC tumors [19, 20]. The lack of copy number data in our series could not help in the

classification of the tumors. Additional limitations of this study include a relatively small sample size, due to the rarity of chRCC, and lack of multiple testing correction. The analysis of TCGA-KICH series support some of the associations, however, further validation should be performed in larger series. In addition, tumor samples availability was limited and IHC for pS6, PTEN, and tuberin derived mostly from tissue microarrays determinations, which can potentially lead to sampling related bias. Furthermore, the relatively low sensitivity and specificity of IHC assays, will limit their use as potential biomarkers.

In conclusion, we provide with novel molecular knowledge on chRCC through the largest series of chRCC tumors so far characterized. Furthermore, we define a subset of cases with mutations activating mTOR pathway, which seems to have aggressive features and poor prognosis, and which may have increased sensitivity to mTOR targeted therapies.

Acknowledgements Human samples used in this project were stored and managed by CNIO-Biobank, as a custody service rendered during the development of the project. We thank the Biobanks of IDIBAPS, IRBLleida (PT13/0010/0014), Santiago, and Complejo Hospitalario Universitario de Vigo, integrated in the Spanish National Biobanks Network, XBTC and SERGAS, together with the collaboration of the Hospital de la Santa Creu i Sant Pau for their collaborative effort. We acknowledge Histopathology Core Unit from CNIO for their great technical support and IHC performance.

Funding This work was supported by the projects RTI2018-095039-B-I00 (Spanish Ministry of Economy, Industry and Competitiveness MEIC/AEI, co-funded by the European Regional Development Fund ERDF), "Club de Atletisme A 4 el KM" from Les Franqueses del Vallés, Young SOGUG Fellowship, "La Caixa" Foundation (ID 100010434) Doctorate in Spain Fellowship Program (LCF/BQ/DE16/11570014), "La Caixa" Foundation INPhINIT—retaining Fellowship Program (LCF/BQ/DR19/11740015), the Spanish Ministry of Education, Culture and Sport "Formación del Profesorado Universitario—FPU" fellowship with ID number FPU2016/05527, Rafael del Pino "Becas de Excelencia" Fellowship, Banco Santander Foundation—CNIO "Fellowships for Young Researchers Trained in the UK/USA" and AECC Foundation grant ID "AIO15152858 MONT".

Compliance with ethical standards

Conflict of interest GdV reports grants from Roche, Pfizer, and Ipsen. Consultancy/Adboard/Honorarium: Novartis, BMS, Janssen, MSD, Astellas, Bayer, Roche, Pfizer, and Ipsen outside the submitted work.

References

1. Rathmell KW, Chen F, Creighton CJ. Genomics of chromophobe renal cell carcinoma: implications from a rare tumor for pan-cancer studies. Oncoscience. 2015;2:81–90.
2. Vera-Badillo FE, Conde E, Duran I. Chromophobe renal cell carcinoma: a review of an uncommon entity. Int J Urol. 2012; 19:894–900.
3. Linehan WM, Ricketts CJ. The Cancer Genome Atlas of renal cell carcinoma: findings and clinical implications. Nat Rev Urol. 2019;16:539–52.
4. Armstrong AJ, Halabi S, Eisen T, Broderick S, Stadler WM, Jones RJ, et al. Everolimus versus sunitinib for patients with metastatic non-clear cell renal cell carcinoma (ASPEN): a multicentre, open-label, randomised phase 2 trial. Lancet Oncol. 2016;17:378–88.
5. Tannir NM, Jonasch E, Albiges L, Altinmakas E, Ng CS, Matin SF, et al. Everolimus versus sunitinib prospective evaluation in metastatic non-clear cell renal cell carcinoma (ESPN): a randomized multicenter phase 2 trial. Eur Urol. 2016;69:866–74.
6. Voss MH, Molina AM, Chen YB, Woo KM, Chaim JL, Coskey DT, et al. Phase II trial and correlative genomic analysis of everolimus plus bevacizumab in advanced non-clear cell renal cell carcinoma. J Clin Oncol. 2016;34:3846–53.
7. Hudes G, Carducci M, Tomczak P, Dutcher J, Figlin R, Kapoor A, et al. Temsirolimus, interferon alfa, or both for advanced renal-cell carcinoma. N Engl J Med. 2007;356:2271–81.
8. Sattler EC, Reithmair M, Steinlein OK. Kidney cancer characteristics and genotype-phenotype-correlations in Birt-Hogg-Dubé syndrome. PLoS ONE. 2018;13:e0209504.
9. Shuch B, Ricketts CJ, Vocke CD, Komiya T, Middelton LA, Kauffman EC, et al. Germline PTEN mutation Cowden syndrome: an underappreciated form of hereditary kidney cancer. J Urol. 2013;190:1990–8.
10. Davis CF, Ricketts CJ, Wang M, Yang L, Cherniack AD, Shen H, et al. The somatic genomic landscape of chromophobe renal cell carcinoma. Cancer Cell. 2014;26:319–30.
11. Ricketts CJ, De Cubas AA, Fan H, Smith CC, Lang M, Reznik E, et al. The Cancer Genome Atlas comprehensive molecular characterization of renal cell carcinoma. Cell Rep. 2018;23:313–26.e5.
12. Casuscelli J, Weinhold N, Gundem G, Wang L, Zabor EC, Drill E, et al. Genomic landscape and evolution of metastatic chromophobe renal cell carcinoma. JCI Insight. 2017;2:e92688.
13. Maroto P, Anguera G, Roldan-Romero JM, Apellániz-Ruiz M, Algaba F, Boonman J, et al. Biallelic TSC2 mutations in a patient with chromophobe renal cell carcinoma showing extraordinary response to temsirolimus. J Natl Compr Cancer Netw. 2018;16: 352–8.
14. Yemelyanova A, Vang R, Kshirsagar M, Lu D, Marks MA, Shih IM, et al. Immunohistochemical staining patterns of p53 can serve as a surrogate marker for TP53 mutations in ovarian carcinoma: an immunohistochemical and nucleotide sequencing analysis. Mod Pathol. 2011;24:1248–53.
15. Köbel M, Ronnett BM, Singh N, Soslow RA, Gilks CB, McCluggage WG. Interpretation of P53 Immunohistochemistry in endometrial carcinomas: toward increased reproducibility. Int J Gynecol Pathol. 2019;38 Suppl 1:S123–31.
16. Grabiner BC, Nardi V, Birsoy K, Possemato R, Shen K, Sinha S, et al. A diverse array of cancer-associated MTOR mutations are hyperactivating and can predict rapamycin sensitivity. Cancer Discov. 2014;4:554–63.
17. Xu J, Pham CG, Albanese SK, Dong Y, Oyama T, Lee CH, et al. Mechanistically distinct cancer-associated mTOR activation clusters predict sensitivity to rapamycin. J Clin Investig. 2016; 126:3526–40.
18. Gopal RK, Calvo SE, Shih AR, Chaves FL, McGuone D, Mick E, et al. Early loss of mitochondrial complex I and rewiring of glutathione metabolism in renal oncocytoma. Proc Natl Acad Sci USA. 2018;115:E6283–90.
19. Chen YB, Mirsadraei L, Jayakumaran G, Al-Ahmadie HA, Fine SW, Gopalan A, et al. Somatic mutations of TSC2 or MTOR characterize a morphologically distinct subset of sporadic renal cell carcinoma with eosinophilic and vacuolated cytoplasm. Am J Surg Pathol. 2019;43:121–31.

20. He H, Trpkov K, Martinek P, Isikci OT, Maggi-Galuzzi C, Alaghehbandan R, et al. "High-grade oncocytic renal tumor": morphologic, immunohistochemical, and molecular genetic study of 14 cases. Virchows Arch. 2018;473:725–38.
21. Guo J, Tretiakova MS, Troxell ML, Osunkoya AO, Fadare O, Sangoi AR, et al. Tuberous sclerosis-associated renal cell carcinoma: a clinicopathologic study of 57 separate carcinomas in 18 patients. Am J Surg Pathol. 2014;38:1457–67.
22. Yang P, Cornejo KM, Sadow PM, Cheng L, Wang M, Xiao Y, et al. Renal cell carcinoma in tuberous sclerosis complex. Am J Surg Pathol. 2014;38:895–909.
23. Zhang Y, Kwok-Shing NgP, Kucherlapati M, Chen F, Liu Y, Tsang YH, et al. A pan-cancer proteogenomic atlas of PI3K/AKT/mTOR pathway alterations. Cancer Cell. 2017;31:820–32.e3.
24. Voss MH, Chen D, Reising A, Marker M, Shi J, Xu J, et al. PTEN expression, not mutation status for TSC1, TSC2 or mTOR, correlates with outcome on everolimus in patients with renal cell carcinoma treated on RECORD-3. Clin Cancer Res. 2019;25:506–14.
25. Roldan-Romero JM, Beuselinck B, Santos M, Rodriguez-Moreno JF, Lanillos J, Calsina B, et al. PTEN expression and mutations in TSC1, TSC2 and MTOR are associated with response to rapalogs in patients with renal cell carcinoma. Int J Cancer. 2020;146:1435–44.
26. Dhawan A, Scott JG, Harris AL, Buffa FM. Pan-cancer characterisation of microRNA across cancer hallmarks reveals microRNA-mediated downregulation of tumour suppressors. Nat Commun. 2018;9:5228.
27. Killela PJ, Reitman ZJ, Jiao Y, Bettegowda C, Agrawal N, Diaz LA, et al. TERT promoter mutations occur frequently in gliomas and a subset of tumors derived from cells with low rates of self-renewal. Proc Natl Acad Sci USA. 2013;110:6021–6.
28. Casuscelli J, Becerra MF, Manley BJ, Zabor EC, Reznik E, Redzematovic A, et al. Characterization and Impact of TERT promoter region mutations on clinical outcome in renal cell carcinoma. Eur Urol Focus. 2019;5:642–9.
29. Grandhi S, Bosworth C, Maddox W, Sensiba C, Akhavanfard S, Ni Y, et al. Heteroplasmic shifts in tumor mitochondrial genomes reveal tissue-specific signals of relaxed and positive selection. Hum Mol Genet. 2017;26:2912–22.
30. Kwiatkowski DJ, Choueiri TK, Fay AP, Rini BI, Thorner AR, de Velasco G, et al. Mutations in TSC1, TSC2, and MTOR are associated with response to rapalogs in patients with metastatic renal cell carcinoma. Clin Cancer Res. 2016;22:2445–52.
31. Palsgrove DN, Li Y, Pratilas CA, Lin MT, Pallavajjalla A, Gocke C, et al. Eosinophilic solid and cystic (ESC) renal cell carcinomas harbor TSC mutations: molecular analysis supports an expanding clinicopathologic spectrum. Am J Surg Pathol. 2018;42:1166–81.
32. Parilla M, Kadri S, Patil SA, Ritterhouse L, Segal J, Henriksen KJ, et al. Are sporadic eosinophilic solid and cystic renal cell carcinomas characterized by somatic tuberous sclerosis gene mutations? Am J Surg Pathol. 2018;42:911–7.